Remote Sensing of Environment 200 (2017) 240–249

Contents lists available at ScienceDirect

Remote Sensing of Environment

journal homepage: www.elsevier.com/locate/rse

Temperature- and texture-dependent dielectric model for frozen and thawed mineral soils at a frequency of 1.4 GHz

Valery L. Mironov[a], Liudmila G. Kosolapova[a,*,1], Yury I. Lukin[a], Andrey Y. Karavaysky[a], Illia P. Molostov[b]

[a] Kirensky Institute of Physics, Federal Research Center KSC SB RAS, Russia
[b] Altai State University, Russia

ARTICLE INFO

Keywords:
Frozen mineral soils
Dielectric measurements
Dielectric model
Unfrozen bound water
Moistened ice
1.4 GHz

ABSTRACT

A single-frequency dielectric model at 1.4 GHz for frozen mineral soils was developed, with the temperature and gravimetric clay content varying from − 1 to − 30°C and from 9.1 to 41.3%, respectively. The model is based on the refractive mixing dielectric model and the dielectric data measured for the three typical soils collected in the Yamal tundra. The refractive mixing dielectric model was applied to fit the measured dielectric data as a function of soil moisture at a number of fixed temperatures. As a result, the parameters of the developed model were derived as a function of temperature and texture. This set of parameters consists of the maximum gravimetric fraction of unfrozen bound water and the values of the complex refractive indexes relating to soil solids, unfrozen bound water, and moistened ice. The developed model for frozen mineral soils in conjunction with the previously developed by us dielectric model for thawed mineral soils is considered as an integral dielectric model which is applicable for permittivity calculations of soil in both thawed and frozen states.

The developed integral dielectric model for frozen and thawed mineral soils was validated using the dielectric data for five measured soils, and the statistical errors were estimated in terms of the root mean square error and the determination coefficient. In addition, the only known in the literature dielectric model for frozen soils suggested by Zhang was validated based on dielectric data for soils measured in this research. The comparative analysis proved substantially better accuracy of predictions in the case of the developed model as compared to those related to the Zhang model.

1. Introduction

1.1. Current state of the problem

Dielectric soil models are used in the development of soil moisture retrieving algorithms based on microwave radiometric and radar data obtained with satellite. In particular, at present dielectric models (Dobson et al., 1985; Mironov et al., 2009) are most successfully used for ***thawed*** soils in the algorithms of SMOS (Soil Moisture Ocean Salinity) and SMAP (Soil Moisture Active Passive). Recently, there has been an interest in using dielectric models for frozen soils. For example, they are applied to explain variations in the radio brightness temperature with a change in the thickness of the frozen soil layer at the temperate latitudes (Zhao et al., 2012) and in subarctic areas (Rautiainen et al., 2012). They are also used in the algorithms for retrieving the temperature profile in the active layer of tundra soils (Mironov et al., 2013d; Mironov et al., 2016). It's probable, that dielectric models for frozen soils can be used in the algorithms for retrieving the moisture of frozen soils, as well as for identifying the frozen/thawed (F/T) state of the upper soil layer. At present, including because of the lack of appropriate dielectric models, the identification of F/T state of the upper soil layer is conducted with the use of the empirical models for radio brightness temperature registered by the remote sensing satellites (Rautiainen et al., 2016; Xu et al., 2016). At the same time, dielectric models for thawed and frozen soils, apparently, could be used to construct more physically based criteria F/T state of soil.

Compared to the thawed soil situation, the available experimental data on frozen soils in the literature are very limited (Zhao et al., 2012). These data give only some idea about the values of frozen soils permittivity, but their number is not sufficient for developing dielectric models. The solution of the problem of developing dielectric models for frozen soils is in the initial stage. Most successfully, this problem is

* Corresponding author at: Kirensky Institute of Physics, Federal Research Center KSC SB RAS, Academgorodok, 50/38, Krasnoyarsk 660036, Russia.
E-mail address: rsdvk@ksc.krasn.ru (L.G. Kosolapova).
[1] Postal mailing address: Kirensky Institute of Physics, Akademgorodok, 50/38, Krasnoyarsk, 660036, Russia.

http://dx.doi.org/10.1016/j.rse.2017.08.007
Received 12 September 2016; Received in revised form 26 June 2017; Accepted 3 August 2017
Available online 18 August 2017
0034-4257/

solved for individual organic soil with organic matter content of 80–90%. Based on the dielectric measurements of this organic soil, a spectroscopic (0.05–15 GHz) (Mironov et al., 2010a) and a single-frequency (1.4 GHz) (Mironov et al., 2015) dielectric models were developed for thawed and frozen soil in the temperature range from − 30°C up to 25°C. The different situation is observed in the case of ***mineral frozen*** soils for which there is still no model based on dielectric measurements. The well-known hypothetical model for frozen mineral soils proposed by Zhang (Zhang et al., 2003), which is a modification of the Dobson model for thawed soils is based on the hypothesis that the complex relative permittivity (CRP) of unfrozen water and ice contained in frozen soil are equal to the CRP values related to the water and ice out of the soil. The amount of unfrozen water is determined by the formulas obtained with the use NMR measurements in (Xu et al., 1985). However, the most substantial disadvantage of the Zhang model is that it still has not been validated with the measured dielectric data. Thus, the problem of developing a dielectric model for frozen mineral soils remains an actual task.

The purpose of this work is to develop a dielectric model for a set of mineral soils with different textures at a frequency of 1.4 GHz based on measured data for frozen soils. This model, in conjunction with the previously developed by us dielectric model for thawed mineral soils (Mironov et al., 2013b), will allow calculations the CRP of mineral soils depending on soil moisture, and soil texture in the temperature range from − 30°C to 25°C. Statistical errors will be estimated for the developed dielectric model for frozen soils with respect to the measured CRP values. In addition, the obtained database for the measured soil CRPs at positive and negative temperatures will be used to estimate the errors of the previously created dielectric model for thawed mineral soils (Mironov et al., 2013b), as well as the dielectric models proposed by Dobson for thawed soils (Dobson et al., 1985) and by Zhang for frozen soils (Zhang et al., 2003). The model being developed in this research uses the same approaches as the other dielectric models developed at the Kirensky Institute of Physics which are briefly reviewed in the next subsection.

1.2. The set of dielectric models developed at the Kirensky Institute of Physics

The set of dielectric models developed at the Kirensky Institute of Physics unites a unified methodology used in their construction. This methodology differs significantly from the approaches used in the previous models (Dobson et al., 1985; Wang and Schmugge, 1980), so that various components of soil water (bound and unbound) are identified based on the dielectric measurements of moist soils. In this case, it is possible to determine the relative content, CRP values, and the parameters of dielectric relaxation for each component of soil water (Mironov et al., 2004). This methodology has made it possible to reduce the error in predicting CRP of moist soils in comparison with previous models (Mironov et al., 2009; Mialon et al., 2015).

A brief review of the dielectric models for thawed mineral soils developed at the Kirensky Institute of Physics is presented in Table 1. This table lists the soils whose dielectric data were used to construct or verify separate models. In addition, the ranges of variation of variables and model parameters are given, namely, the texture of soils, moisture, temperature, frequency of the electromagnetic field. The soils texture is characterized only by the percentage of the clay content in the soil, determined by the USDA classification. As it was shown in work (Mironov et al., 2009) based on the data of dielectric and granulometric measurements, it is this value which has the most effect on the CRP of moist soils.

Based on the dielectric model for individual soil and the measured data of dielectric spectra for 15 soils with different clay content varying over a wide range, a new texture-dependent spectroscopic, dielectric model was developed at a fixed temperature of ~20°C (Mironov et al., 2009). The next stage in the development of the moist soils dielectric models created at the Kirensky Institute of Physics was devoted to taking into account the dependence of the soil CRP on temperature. At the first stage, a technique was proposed for developing a temperature-dependent dielectric model for individual soils (Mironov and Fomin, 2009a). Later on, a temperature- and texture-dependent dielectric model (Mironov & Fomin, 2009b) was created based on dielectric models that take into account the soil CRP dependence on soil texture (Mironov et al., 2009), and temperature (Mironov and Fomin, 2009a) using dielectric data for 15 soil types measured in the temperature range from 10 to 40°C (Curtis et al., 1995). In all the spectroscopic dielectric models considered above, only the dipole Debye relaxation for soil water molecules was taken into account. It was found, that the error in predicting the CRP of moist soils with the help of these dielectric models increased significantly in the megahertz frequency range. It was shown in (Mironov et al., 2013a), that by taking into account in the spectroscopic model for the individual soil (Mironov et al., 2004) not only the dipole relaxation, but also the Maxwell-Wagner ionic relaxation for bound water, it was possible to obtain a prediction error of the soil CRP in the megahertz range comparable to the prediction error in the gigahertz frequency range. As a result, a multi-relaxation spectroscopic dielectric model for individual soil was developed.

Since in some applications of soil, dielectric models for remote sensing problems it is sufficient to predict the values of soil CRP at fixed frequencies, single-frequency dielectric models of moist soils are also developed at the Kirensky Institute of Physics. Methodically, these models are based on the use of a refractive dielectric model of a mixture which parameters are determined directly from the dielectric measurements of moist soils. In contrast to spectroscopic dielectric models, the single-frequency models are much simpler in methodology in developing and more convenient for practical use. Such a model was created based on dielectric measurements in (Curtis et al., 1995) and it allows to calculate the permittivity of thawed mineral soils depending on moisture, temperature, and texture at 1.4 GHz (Mironov et al., 2013b). The works presented in Table 1 can be divided into two groups. The first group includes the works that develop a methodology for constructing dielectric models of moist soils (Mironov et al., 2004; Mironov and Fomin, 2009a; Mironov et al., 2013a). The second group includes the models (Mironov et al., 2009b; Mironov & Fomin, 2009b;Mironov et al., 2013b), suitable for practical use in the algorithms of radio-thermal and radar remote sensing.

2. Characterization of the measured soils and dielectric measurement technique

To develop the dielectric model we measured the three basic soils collected in Yamal peninsula, Russia (soils 1, 2, 3 in Table 2). Two more soils we measured for independent validation of the developed dielectric model (soils 4 and 5 in Table 2). As seen from Table 2, mineral compositions of the basic soils are rather close to each other, while, their textures in term of clay content vary in the range from 9.1 to 41.3%. Dielectric measurements for soils were carried out in the frequency range from 0.05 to 15 GHz for the soil moistures from zero to field capacity, with the temperature changing from − 30 to 25 °C. For development and validation of the dielectric model, only the dielectric data at the frequency of 1.4 GHz were used.

To obtain samples in the moisture range less than the hygroscopic moisture, soil was dried in an oven at 104°C for 6 h. The sample with minimal content water was placed immediately after drying into the measuring container. The other samples in this range of moistures were obtained by keeping the dried soil in open air during different time intervals. To obtain samples with moistures greater than the hygroscopic moisture of soil, varying portions of distilled water were added into soil samples by calibrated pipette. The prepared samples were mixed well and stored in a sealed container at least for one day. To conduct dielectric measurement, the soil sample was placed into a cell

Table 1
Brief description of the dielectric models created by the Kirensky Institute of Physics for thawed mineral soils.

Thawed mineral soils						
Paper	Measured soils	Texture (clay content, %)	Moisture	Temperature, °C	Frequency, GHz	Comments
1. Mironov et al., 2004	Sand, bentonite in (Mironov et al., 2004) Field 1, Field 5 in (Dobson et al., 1985)	0; 51.5 13.43; 47.38	Volumetric moisture from 0 to field capacity	0; 25 20–22	0.6; 1.1; 1.43 4; 10; 18	***New methodology*** of dielectric model development for individual soil (Methodical)
2. Mironov et al., 2009	15 soils in (Curtis et al., 1995)	0–76		20–22	0.3–26.5	Spectroscopic, ***texture*** dependent dielectric model (Model for users)
3. Mironov and Fomin, 2009a	Silty sand soil in (Curtis et al., 1995)	14		10–40	0.3–26.5	Spectroscopic, ***temperature*** dependent dielectric model for individual soil (Methodical)
4. Mironov and Fomin, 2009b	5 soils in (Curtis et al., 1995)	0; 14; 34; 54; and 76		10–40	0.3–26.5	Spectroscopic, ***temperature***, and ***texture*** dependent dielectric model (Model for users)
5. Mironov et al., 2013a	Silty sand soil, Gray clay soil in (Curtis et al., 1995) Silty clay loam in (Wagner et al., 2011)	4 34 29.7		20	0.4–26.5	***Multi-relaxation***, spectroscopic, dielectric model for individual soil (Methodical)
6. Mironov et al., 2013b	15 soils in (Curtis et al., 1995)	0–76		10–40	1.4	***Single-frequency***, texture, and temperature dependent dielectric model (Model for users)

formed by a section of coaxial waveguide with the cross section of 7/3 mm, the latter ensuring that only TEM mode is present in the measured frequency range. The length of sample placed in the cell and its volume were equal to 17 mm and 0.529 cm^3, respectively.

When filling the measuring cell, the soil was compacted with a cylinder pestle. The cell was blocked on both sides with teflon washers, which prevented the sample from changing in volume. The measuring cell was connected to the ZVK Rohde & Schwarz or Agilent vector network analyzers to measure the frequency spectra of the S11, S22, S12, and S21 elements of the scattering matrix S over the frequency range from 0.05 to 15 GHz. The isothermal measurements were ensured with the use of an SU-241 Espec chamber of heat and cold. To control the isothermal measurements, a combined system consisting of the chamber and the network analyzer was developed, using the RS-232 interface and a set of built in commands. This system allows setting a sequence of temperatures at which the spectra of the scattering matrix are measured isothermally. After the temperature control system switches the chamber to a next assigned temperature point the system starts controlling the root mean square deviations between the values of S12 spectra consequently measured every second. After the value of the root mean square deviation decreases to below 0.01 the elements S11, S22, S12, and S21 are recorded. After recording is over the system switches the chamber to the next assigned temperature point, and the process of establishing temperature equilibrium between the sample and the chamber at the assigned temperature point repeats. A time interval to transfer from one measurement temperature to another is maximal at the larger moistures of frozen soil sample, which take the following values: 40 min and 20 min in the case of frozen soil for the temperature intervals $-15\,°C < T < -1\,°C$ and $-30\,°C < T < -15\,°C$, respectively. The algorithm developed in (Mironov et al., 2010b; Mironov et al., 2013c) was applied to retrieve the CRP spectra of the moist samples using the measured values of S11 and S12 or S22 and S21. This algorithm provides the real and imaginary parts of the CRP of moist samples with the errors < 10% and 20%, respectively.

Table 2
Soil texture parameters and mineral composition.

No.	Soil type	Location	Soil texture (%)				Mineral composition				
			Sand	Silt	Clay	Organic matter	Quartz (%)	Feldspar (%)	Plagio clase (%)	Mica, chlorite (small impurity)	Smectite, Amphibol, Siderite (traces)
1	Sandy loam	Yamal N 70°16′ 31″ E 68°53′30″	41.4	49.5	9.1	0.9	40	30	30	Imp.	Tr.
2	Silt loam	Yamal N 70°18′05″ E 68°50′29″	40.4	39.0	20.6	2.1	70	15	5–10	Imp.	Tr.
3	Silty clay	Yamal N 70°16′52″ E 68°53′29″	1.6	57.1	41.3	2.3	60	20–25	5	Imp.	Tr.
4	Clay loam	Krasnodar N45°02′41″ E38°58′33″	20.6	46.0	33.4	4.1	60	10	15	5–10	Tr.
5	Silty clay	Yamal N 70°17′48″ E 68°54′12″	2.0	55.8	42.2	3.2	55–60	10	15–20	5–7	2–3

Table 3
Soil samples gravimetric moistures, m_g [g/g], and their respective bulk densities, ρ_d [g/cm^3].

Soil 1	m_g	0.004	0.005	0.012	0.023	0.039	0.047	0.052	0.061	0.072	0.091	0.096	0.101	0.117
	ρ_d	1.62	1.60	1.65	1.54	1.48	1.51	1.53	1.55	1.49	1.53	1.55	1.57	1.58
	m_g	0.135	0.156	0.165	0.182									
	ρ_d	1.65	1.86	1.67	1.65									
Soil 2	m_g	0.004	0.025	0.040	0.058	0.064	0.068	0.071	0.093	0.111	0.132	0.138	0.143	0.154
	ρ_d	1.52	1.36	1.41	1.29	1.33	1.36	1.34	1.43	1.44	1.45	1.50	1.55	1.46
	m_g	0.171	0.180	0.192	0.209	0.211								
	ρ_d	1.83	1.48	1.80	1.63	1.62								
Soil 3	m_g	0.004	0.047	0.058	0.061	0.066	0.077	0.080	0.085	0.097	0.111	0.129	0.136	0.144
	ρ_d	1.30	1.40	1.32	1.34	1.28	1.36	1.36	1.38	1.40	1.48	1.57	1.44	1.49
	m_g	0.154	0.164	0.182	0.205	0.233	0.236	0.263	0.274	0.280	0.289	0.298	0.300	0.315
	ρ_d	1.48	1.54	1.55	1.59	1.59	1.63	1.54	1.52	1.50	1.49	1.44	1.46	1.42

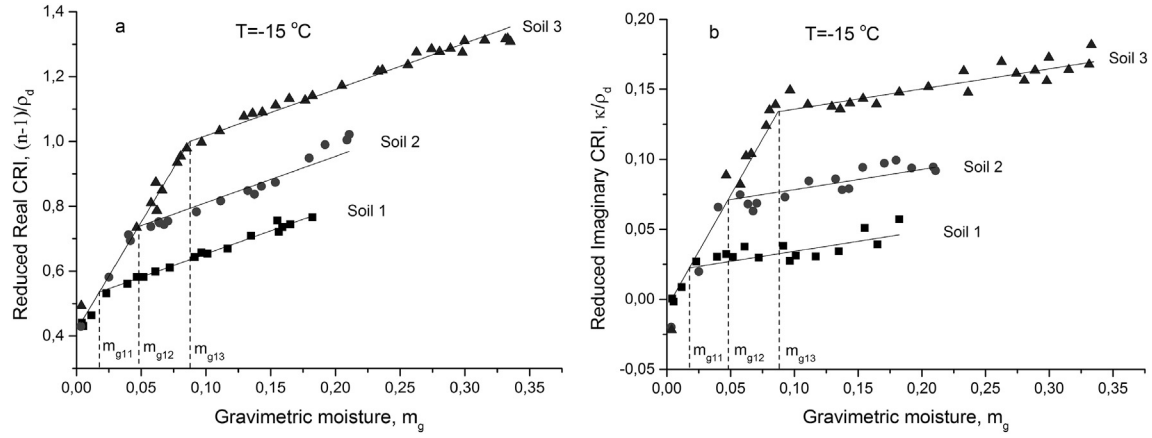

Fig. 1. The reduced complex refractive index of the measured soils (symbols) at the temperature of − 15 °C and wave frequency of 1.4 GHz as a function of gravimetric moisture. a) The reduced real part of the CRI, b) the reduced imaginary part of the CRI.

3. Dielectric model

3.1. Model description

The model for frozen soils was developed on the bases of our dielectric measurements. In Table 3, the values of gravimetric moistures and bulk densities for the measured soil samples are given. The values of given soil bulk densities lie in the same intervals (a normal range of bulk densities for clay is 1.0 to 1.6 mg/m^3 and a normal range for sand is 1.2 to 1.8 mg/m^3) as those observed in situ (Aubertin and Kardos, 1965). Using these data, the volumetric moistures, m_v, of the measured samples can be easily estimated, $m_v = m_g\,\rho_d/\rho_w$. ρ_w is density of water and $\rho_w = 1$ g/cm^3.

As can be seen from Table 3, each soil sample corresponding to fixed moisture has its own bulk density. Varying values of bulk density in the measured soil samples arise when the soil substance, having different amounts of water, is packed into a measuring coaxial cell. Like in (Mironov et al., 2010a), the reduced values of the real, $(n_s - 1)/\rho_d$, and imaginary, κ_s/ρ_d, parts of the soil complex refractive index (CRI) are used in formulation of the developed dielectric model with formulas (1) and (2). Formulas (1) and (2) are based on the refractive mixing dielectric model (RMDM) (Mironov et al., 2010a). As can be seen from formulas (1) and (2), the reduced CRI does not depend on soil bulk density, ρ_d, because the right parts in formulas (1) and (2) do not contain the values of soil bulk densities.

$$\frac{n_s-1}{\rho_d}=\begin{cases}\frac{n_m-1}{\rho_m}+\frac{n_b-1}{\rho_b}m_g & m_g\le m_{g1}\\ \frac{n_m-1}{\rho_m}+\frac{n_b-1}{\rho_b}m_{g1}+\frac{n_i-1}{\rho_i}(m_g-m_{g1}) & m_g\ge m_{g1}\end{cases} \quad (1)$$

$$\frac{k_s}{\rho_d}=\begin{cases}\frac{k_m}{\rho_m}+\frac{k_b}{\rho_b}m_g & m_g\le m_{g1}\\ \frac{k_m}{\rho_m}+\frac{k_b}{\rho_b}m_{g1}+\frac{k_i}{\rho_i}(m_g-m_{g1}) & m_g\ge m_{g1}\end{cases} \quad (2)$$

The subscripts s, d, m, b, and i (which are related to n, κ, and ρ) refer to the moist soil, dry soil, solid (mineral) component of soil, unfrozen bound water, and moistened ice, respectively. m_{g1} is the maximum gravimetric fraction of unfrozen bound water at a fixed temperature. In (Mironov et al., 2010a) three components of water in frozen ***organic*** soil, namely bound water, transient bound water and moistened ice, appeared to be identified, and related amounts of each water component were determined from dielectric measurements. In frozen ***mineral*** soils, our measurements allowed to identify only two components of soil water, namely, unfrozen bound water and moistened ice. At that, the unfrozen bound water is supposed to include bound water and transient bound water as they were earlier introduced in (Mironov et al., 2010a). The real, ε_s', and imaginary, ε_s'', parts of the soil CRP are expressed through the real, n_s, and imaginary, κ_s, parts of the CRI introduced by formulas (1), and (2) in the following form:

$$\varepsilon_s' = n_s^2 - \kappa_s^2, \quad \varepsilon_s'' = 2n_s\kappa_s. \quad (3)$$

A number of moisture dependencies of the reduced CRIs were measured for the frozen soil samples at the wave frequency of 1.4 GHz and at fixed temperatures, T, which values ranged from − 30 to − 1°C. Some of those measured dependencies are shown with symbols in Fig. 1. The values of m_{g11}, m_{g12}, and m_{g13} that separate the range of unfrozen bound water from that of moistened ice for basic soils (soil 1, soil 2, soil 3 from Table 1) are marked herein with vertical dashed lines. Along with the measured data, the best fits obtained with the use of the

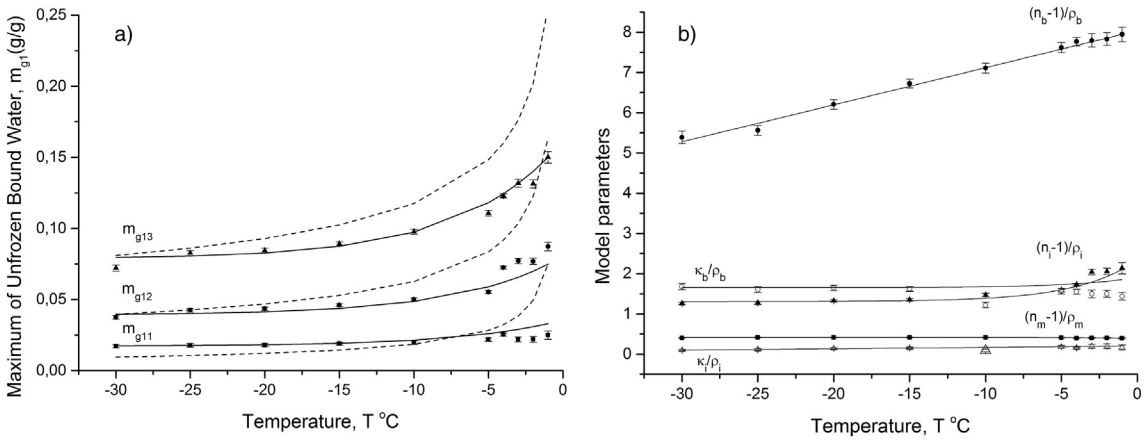

Fig. 2. The model parameters together with the standard errors: a) m_{g11}, m_{g12}, and m_{g13} are as the functions of temperature and texture (clay content), solid lines correspond to the being developed model, and dashed lines correspond to the Zhang model, b) the other parameters of the being developed model are as functions of temperature.

RMDM (1)–(2) are also presented in Fig. 1. In the process of fitting the software ORIGIN 9.0 was applied. The mode of Global Fitting was used which suggest simultaneous fitting datasets for the three measured soils with the same fitting functions (1)–(2). The parameters $((n_m - 1)/\rho_m, \kappa_m/\rho_m)$, $((n_b - 1)/\rho_b, \kappa_b/\rho_b)$, and $((n_i - 1)/\rho_i, \kappa_i/\rho_i)$ in the fitting functions were shared amongst all datasets, while parameters m_{g11}, m_{g12}, and m_{g13} were uniquely determined for the datasets concerning each soil. When using such a mode of fitting the maximum gravimetric fractions of the unfrozen bound water, m_{g1}, is suggested to depend on both texture and temperature of soil. While the reduced CRI's of solid component, $((n_m - 1)/\rho_m, \kappa_m/\rho_m)$, unfrozen bound water, $((n_m - 1)/\rho_m, \kappa_m/\rho_m)$, and moistened ice, $((n_i - 1)/\rho_i, \kappa_i/\rho_i)$, of the measured soils are considered to be independent on soil texture. The above fitting procedure was performed for the measured data obtained at the temperatures of − 1, − 2, − 3, − 4, − 5, − 10, − 15, − 20, − 25, − 30 °C. The values of parameters m_{g11}, m_{g12}, and m_{g13} at the fixed measured temperature resulting from this fitting are shown with symbols in Fig. 2a. While the values of the RMDM parameters $((n_m - 1)/\rho_m, \kappa_m/\rho_m)$, $((n_b - 1)/\rho_b, \kappa_b/\rho_b)$, and $((n_i - 1)/\rho_i, \kappa_i/\rho_i)$ are shown as a function of temperature with symbols in Fig. 2b. Further, the datasets for m_{g1} (T, C) were fitted as a function of temperature using the fitting function $m_{g1}(T, C) = A(C)(1 + B\exp(T/T_d))$. Parameters B and T_d in the fitting function were shared amongst all datasets obtained for the three soils, while parameter A(C) was uniquely determined for each soil. The values of A(C) were finally fitted by a linear function of clay content C. The maximum gravimetric fraction of unfrozen bound water, m_{g1}, as a function of temperature and clay content (T, C), resulting from the last two fittings is given by the formula (4). The solid lines in Fig. 2a represent the results of calculations obtained with this formula. According to this formula, the quantity of unfrozen bound water is proportional to the clay content in soil at all the measured temperatures. In particular, at the temperature − 30 °C the maximum gravimetric fraction of unfrozen bound water is approaching to the value of 0.0019C.

Let us analyze the parameters $(n_m - 1)/\rho_m$ and κ_m/ρ_m, $((n_b - 1)/\rho_b$ and $\kappa_b/\rho_b)$ $((n_i - 1)/\rho_i$ and $\kappa_i/\rho_i)$ shown by symbols in Fig. 2b. In their tune, the datasets shown in Fig. 2b were fitted as a function of temperature with linear and exponential functions, which are shown by solid lines.

The formulas for best fits are given in (4)–(10).

$$m_{g1} = 0.0019C\,(1 + 1.056\,\exp(T/6.77)), \tag{4}$$

$$(n_m - 1)/\rho_m = 0.415–0.0256\,\exp(T/3.57), \tag{5}$$

$$(n_b - 1)/\rho_b = 8.042 + 0.0921T, \tag{6}$$

$$(n_i - 1)/\rho_i = 1.305 + 1.022\,\exp(T/4.02), \tag{7}$$

$$\kappa_m/\rho_m = 0, \tag{8}$$

$$\kappa_b/\rho_b = 1.654–0.258\,\exp(T/4.07), \tag{9}$$

$$\kappa_i/\rho_i = 0.204 + 0.00354T. \tag{10}$$

Finally, we obtained the temperature- and texture-dependent dielectric model for the CRP of frozen mineral soils at the frequency of 1.4 GHz, which is expressed with formulas (1)–(10). To calculate the CRP as a function of gravimetric moisture or as a function of temperature using formulas in (1)–(10), one must assign the following variables: 1) dry soil density, ρ_d [g/cm^3], 2) gravimetric moisture, m_g [g/g], 3) temperature, T °C, and 4) clay content in soil, C in %.

3.2. Permittivity of unfrozen bound water and moistened ice

Assuming ρ_b and ρ_i equal to 1 g/cm^3 in formulas (4)–(10) one can determine the permittivity of unfrozen bound water and moistened ice as a function of temperature.

$$\varepsilon'_b = 79.02 + 1.666T + 0.0001T^2 + 0.853\,\exp(T/4) - 0.0666\,\exp(T/2), \tag{11}$$

$$\varepsilon''_b = 29.91 + 0.305T - 4.666\,\exp(T/4) - 0.0475T\,\exp(T/4), \tag{12}$$

$$\varepsilon'_i = 5.27–0.0014T–1.25\cdot10^{-5}T^2 + \exp(T/2) + 4.61\exp(T/4), \tag{13}$$

$$\varepsilon''_i = 0.94 + 0.016T + 0.408\,\exp(T/4) + 0.00708T\,\exp(T/4). \tag{14}$$

Fig. 3 shows ε'_b and ε''_b, ε'_i and ε''_i depending on the temperature calculated by the formulas (11)–(14).

According to our calculations of unfrozen bound water decreases from 80 to 36, when the temperature changes from − 1 °C to − 30 °C. At the same time, the dielectric constant of moistened ice varies with decreasing temperature from 9 to 5. In dielectric models (Wang and Schmugge, 1980; Dobson et al., 1985) permittivity of ice are considered equal to 3.15 + i0. Since in our calculation we obtained significantly larger values for the dielectric constant of ice in frozen soil, we consider that ice in the frozen soil may be a mixture of crystalline ice and adsorbed liquid water.

In the following sections, the developed model will be validated by comparing the calculated CRP values with the respective measured ones. In addition there will be conducted a comparative analysis of the errors relating to the developed model and the Zhang model (Zhang et al., 2003; Zhang et al., 2010) for frozen mineral soils. Besides, the dielectric data measured in this research will be used for validation of the dielectric models for thawed mineral soils which were previously developed by us (Mironov et al., 2013b) and Dobson (Dobson et al., 1985).

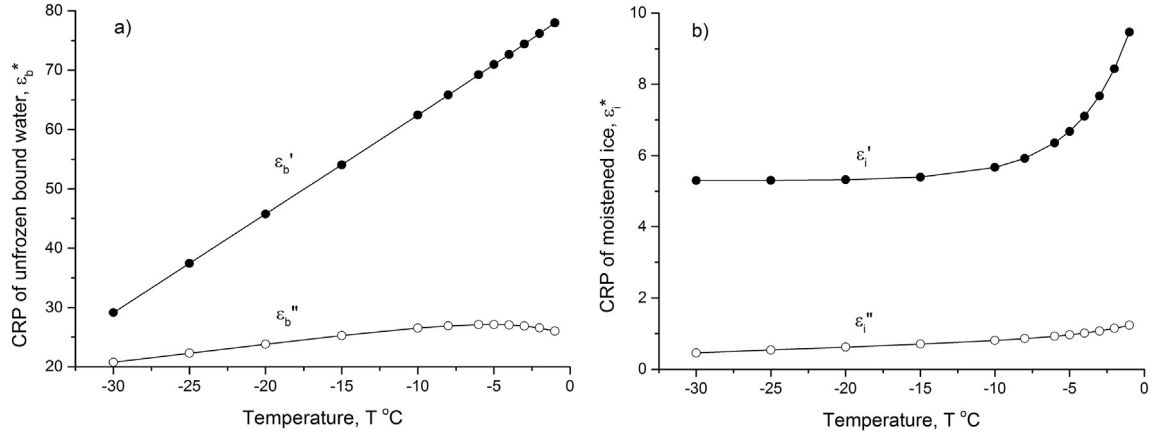

Fig. 3. Complex relative permittivity as functions of temperature in frozen mineral soils for a) unfrozen bound water and b) moistened ice.

Table 4
Soil samples gravimetric moistures, m_g [g/g], bulk densities, ρ_d [g/cm^3], volumetric moistures m_v[cm^3/cm^3] used for models validation in Figs. 4, and 5.

	Basic soils						Independent soils			
	Soil 1		Soil 2		Soil 3		Soil 4		Soil 5	
m_g	0.047	0.160	0.068	0.210	0.046	0.256	0.120	0.217	0.075	0.397
ρ_d	1.51	1.86	1.36	1.63	1.40	1.58	1.64	1.66	1.25	1.28
m_v	0.07	0.29	0.09	0.34	0.065	0.40	0.19	0.36	0.10	0.51

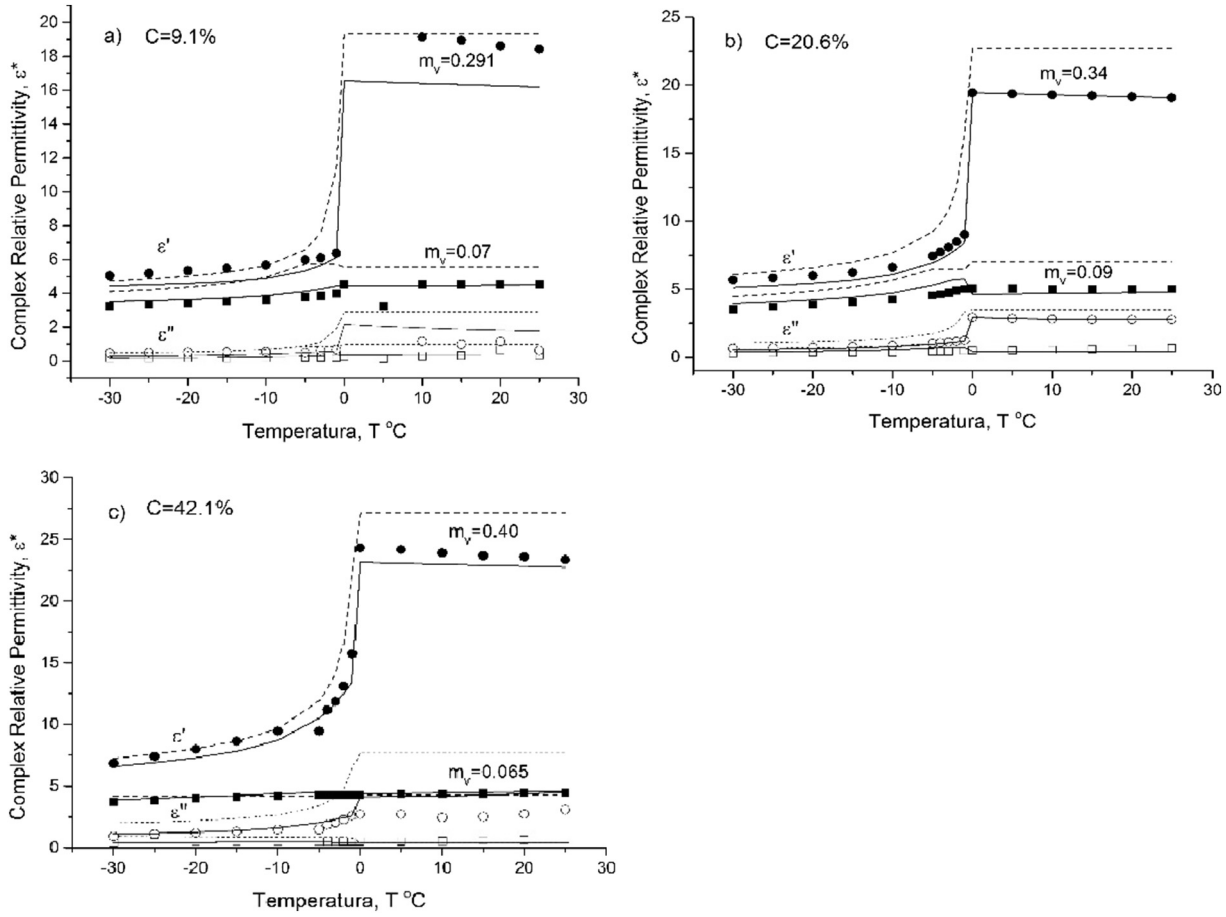

Fig. 4. Comparison of CRPs between calculated and measured values for basic soils. The CRPs of moist soil as a function of temperature at the fixed volumetric moistures m_v (given by inscriptions). a) The CRPs of soil 1, b) the CRPs of soil 2, c) the CRPs of soil 3. The measured CRP values are represented by symbols. The solid lines correspond to the CRPs estimated with the developed model ($T < 0$) and earlier developed model ($T \geq 0$). The dash lines correspond to the CRPs calculated with the Zhang model ($T < 0$) and Dobson ($T \geq 0$).

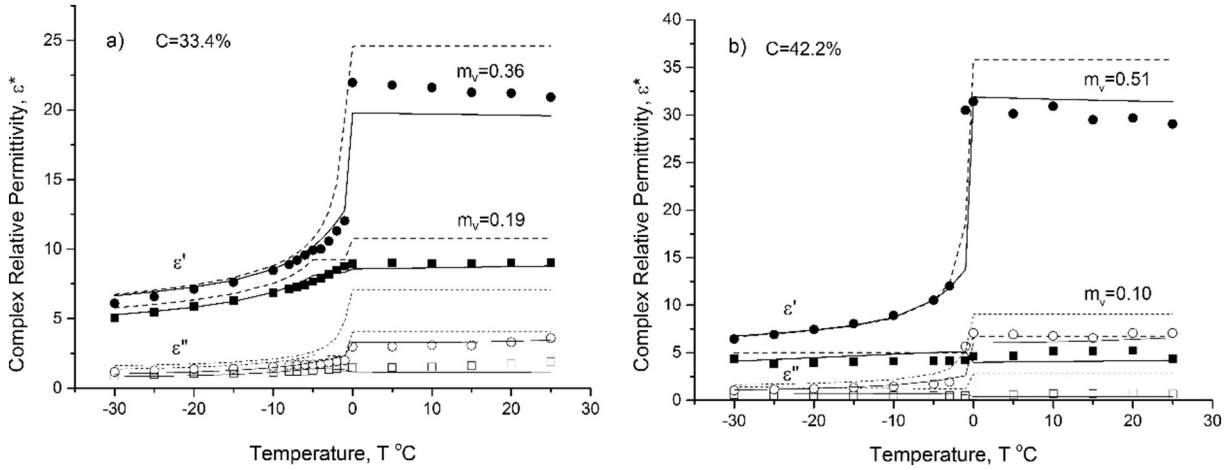

Fig. 5. Comparison of CRPs between calculated and measured values for independent soils. The CRPs of moist soil as a function of temperature at the fixed volumetric moistures m_v (given by inscriptions) and the frequency of 1.4 GHz. a) The CRPs of soil 4, b) the CRPs of soil 5 (see Tables 2, and 4). The designations are the same as in Fig. 4.

4. Validation of the developed dielectric model

The developed model concerning the frozen soils was validated with the use of the dielectric data measured for the three basic soils, which were used for developing model, and two independent soils, which measured dielectric data were not used for developing this model. As an example, in Fig. 3 the results of the measurements conducted in this research for the basic soils 1, 2, and 3 (see Table 2) are shown as a function of temperature at two fixed moistures (see Table 4), together with the respective predictions obtained with the use of the developed model for frozen soils. As can be seen from Fig. 4, good correlation is observed between the measured data and the ones calculated with the developed model.

As seen from Fig. 5, good agreement between the values predicted with the developed dielectric model for frozen soils and the respective measured values are also observed for the soils which were especially measured for validation purpose (soils 4, 5 in Table 2).

Further, a quantitative analysis for the statistical errors of the developed dielectric model for frozen soils was conducted relative to the respective measured dielectric values. Calculated with the developed model the real and imaginary parts of the CRP for the two independent soils (soil 4, and soil 5, see Table 2) are shown as a function of measured data in Fig. 6a, b, respectively. At that, the data given in Fig. 6 include the dielectric data for the soil samples, with the values of moistures evenly distributed between the lowest and highest measured values of moisture. The total number of data used for estimations of statistical errors was equal to 129.

Good correlation between the soil CRP values calculated with the developed model (filled circles) and the measured ones is observed herein. Estimations of the statistical errors for the developed dielectric model were conducted in terms of root mean square error (RMSE), normalized RMSE (n RMSE), and determination coefficient (R^2). For this purpose, the following formulas were used.

$$RMSE = \sqrt{\sum_{i=1}^{n} \frac{(x_i - y_i)^2}{n}},$$

$$\mathrm{RMSE} = \sqrt{\sum_{i=1}^{n} \frac{(x_i - y_i)^2}{n}} \quad \text{nomalized RMSE} = \frac{\sqrt{\frac{\sum_{i=1}^{n}(x_i - y_i)^2}{n}}}{\overline{x}} \cdot 100\%,$$

$$R^2 = 1 - \frac{\sum (x_i - y_i)^2}{\sum (x_i - \overline{x})^2}$$

where x_i, y_i, $\overline{x}$ are measured values, predicted values, and the average measured value, respectively; n is number of measurements. The results of error estimations are given in Table 5.

As can be seen from Table 5, the values of nRMSE for the real and imaginary parts of soil CRPs

are closed to the ones of the dielectric measurements.

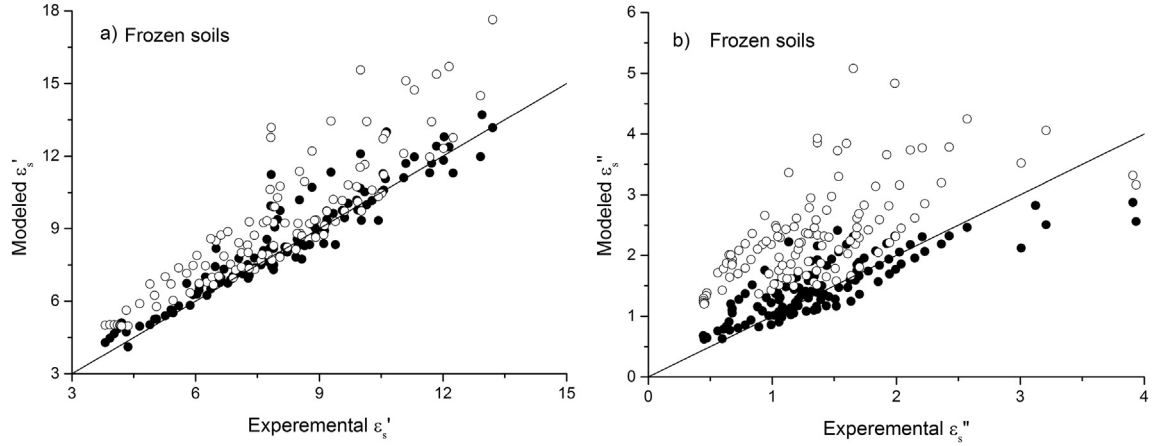

Fig. 6. The calculated CRPs of moist soils as a function of the measured ones for independent soils a) the real part of CRPs, ε_s', b) the imaginary part of CRPs, ε_s'', in the temperature ranges of $-30\ ^\circ\mathrm{C} \le T \le -1\ ^\circ\mathrm{C}$. Bisectors represented by the lines. Filled circles represent the model (1)–(10), empty circles represent Zhang model.

Table 5
Statistical errors for the developed model (***Mir***) and the Zhang Model (***Zha***) in the case of frozen soils.

	Independent soils, $T < 0$					
	RMSE		nRMSE, %		R^2	
	Mir	Zha	Mir	Zha	Mir	Zha
ε_s'	0.76	2.16	9.42	26.9	0.89	0.60
ε_s''	0.36	1.18	26.26	85.50	0.53	0.19

5. Comparative analysis of the errors related to the developed model and the Zhang model

Before conducting the comparative analysis of the errors related to the developed model and the known in the literature Zhang model (Zhang et al., 2003; Zhang et al., 2010) for frozen soils the formulation of the Zhang model is given. Because, some uncertainties contained in the original papers need to be clarified.

5.1. Zhang model

The Zhang model is an extension of the Dobson model for the case of frozen soils. The Zhang model is presented herein based on the formulation of the Dobson model given in (Mironov et al., 2009). The extended for the frozen soils the Dobson dielectric model can be written in the following way:

$$\varepsilon_f' = \left[1 + \frac{\rho_b}{\rho_s}(\varepsilon_s'^{\alpha} - 1) + m_{vu}^{\beta'}\varepsilon_{uw}'^{\alpha} - m_{vu} + m_{vi}\varepsilon_i'^{\alpha} - m_{vi}\right]^{1/\alpha}, \tag{15}$$

$$\varepsilon_f'' = [m_{vu}^{\beta''}\varepsilon_{uw}''^{\alpha}]^{1/\alpha}, \tag{16}$$

where ε'_s is a real part of CRP of the soil solids; m_{vu}, and m_{vi} are the volumetric moisture contents of unfrozen water and ice, respectively; ρ_b is the bulk density in g/cm^3, ρ_s is the specific gravity of the soils. $\alpha = 0.65$ is an empirically determined constant, and β' and β'' are empirically determined soil texture dependent parameters given by:

$$\beta' = 1.2748 - 0.00519\ S - 0.00152\ C, \tag{17}$$

$$\beta'' = 1.33797 - 0.00603\ S - 0.00166\ C, \tag{18}$$

where S and C are percentages by weight of sand and clay, respectively. The quantities ε'_{uw} and ε''_{uw} are the real and imaginary parts of CRP of unfrozen water, given by the modified Debye equations:

$$\varepsilon_{uw}' = \varepsilon_{w\infty} + \frac{\varepsilon_{w0} - \varepsilon_{w\infty}}{1 + (2\pi f\tau_w)^2}, \tag{19}$$

$$\varepsilon_{uw}'' = \frac{2\pi f\tau_w(\varepsilon_{w0} - \varepsilon_{w\infty})}{1 + (2\pi f\tau_w)^2} + \frac{\sigma_{eff}}{2\pi\varepsilon_0 f}\frac{(\rho_s - \rho_b)}{\rho_s m_v} \tag{20}$$

where ε_0 is the dielectric constant of free space, which is equal to 8.854×10^{-12} F/m, τ_w is the relaxation time for unfrozen water, f is the frequency in Hz, ε_{w0} and $\varepsilon_{w\infty} = 4.9$ are the low and high frequency limits of the dielectric constant for unfrozen water, respectively. σ_{eff} is the effective conductivity of unfrozen water which is determined in the following form:

$$\sigma_{eff} = -1.645 + 1.939\ \rho_b - 0.0225622\ S + 0.01594\ C \tag{21}$$

In the original publications regarding the Zhang model, there was recommended to use the temperature dependences for the static dielectric constant, ε_{w0}, and the relaxation time, τ_w, of unfrozen water in frozen soils, which were obtained for the liquid water in the range of positive temperatures ($T \geq 0$ °C). However, any references to make these temperature dependences available were not distinctly pointed out in (Zhang et al., 2003; Zhang et al., 2010). To resolve this uncertainty the respective formulas for temperature dependencies for the static dielectric constant, ε_{w0}, and the relaxation time, τ_w, of unfrozen water the formulas, which were obtained in (Stogryn, 1971) for liquid water at the positive temperatures ($T \geq 0$ °C) are applied:

$$2\pi\tau_w = 1.1109\cdot10^{-10} - 3.824\cdot10^{-12}T + 6.938\cdot10^{-14}T^2 - 5.096\cdot10^{-16}T^3 \tag{22}$$

$$\varepsilon_{w0} = 87.74 - 0.40008T + 9.398\cdot10^{-4}T^2 + 1.410\cdot10^{-6}T^3. \tag{23}$$

The same values as in (Zhang et al., 2003) for other key parameters $\varepsilon_s = 4.70 - i0$ and $\varepsilon_i = 3.15 - i0$ are used.

To determine the amount of unfrozen water in the soil as a function of soil temperature the formulas from (Xu et al., 1985) were used:

$$m_{vu} = a\ |T_s|^{-b}\ \rho_b/\rho_w \tag{24}$$

$$\ln\ a = 0.5519\ \ln\ SSA + 0.2618,\ \ln\ b = -0.264\ \ln\ SSA + 0.3711, \tag{25}$$

where m_{vu}, T_s, and SSA are volumetric content of unfrozen water (cm^3/cm^3), soil temperature (°C), specific surface area (m^2/g), respectively. An equation for predicting SSA was established in (Ersahin et al., 2006):

$$SSA = 0.042 + 4.23clay\% + 1.12silt\% - 1.16sand\%. \tag{26}$$

The volumetric content of ice m_{vi} in frozen soils is expressed as

$$m_{vi} = m_v - m_{vu}, \tag{27}$$

where m_v is a volumetric total water content in soil. At the same time, formula (3) in (Zhang et al., 2003) for the volumetric content of ice, m_{vi}, appeared to be incorrect. To be sure that we have correctly understood and interpreted the Zhang model outlined in (Zhang et al., 2003; Zhang et al., 2010), we calculated the CRP values for the three specific soils using formulas (15)–(27). Earlier, these calculations were performed by the authors of the Zhang model and the results are available in Fig. 2 in (Zhang et al., 2003). The results of our calculations with formulas (15)–(27) were found to be in perfect agreement with the results in Fig. 2 in (Zhang et al., 2003). Further, we will validate the Zhang model on the bases of dielectric data for frozen soils measured in this research.

5.2. Results of the comparative analysis

Comparison between measured values and the CRP values calculated with the Zhang model are shown in Fig. 4, 5, and 6. As a whole, the values of soil CRPs calculated with the developed model correlate substantially better with the respective measured values than those calculated with the Zhang model. Clouse values calculated with the developed model and the Zhang model are observed only for real parts of the soil CRPs at the temperatures less than −10 °C. Quantitative estimations of the statistical errors for the Zhang model are given in Table 5. As can be seen from Table 5, the values of RMSE and nRMSE for the real and imaginary parts of the soil CRPs concerning the Zhang model are greater by the factor of about 3 in comparison with the same values concerning the developed model.

6. Comparative analysis of the errors related to the Dobson and Mironov models at positive temperatures

Let's consider, an assemblage of the developed model for frozen mineral soils and the previously developed model (Mironov et al., 2013b) for thawed mineral soils as an integral single-frequency dielectric model for mineral soils at positive and negative temperatures. Similarly, an assemblage of the Zhang model for frozen soils (Zhang et al., 2003, 2010) in conjunction with the Dobson model for thawed soils (Dobson et al., 1985) can be considered as another integral dielectric model in the range of both negative and positive temperatures. In this section, the previously developed model (Mironov et al., 2013b) and the Dobson model (Dobson et al., 1985) for thawed soils will be validated regarding the dielectric data for the five soils measured in this research (see Table 2). Note, that these measured data were not used for

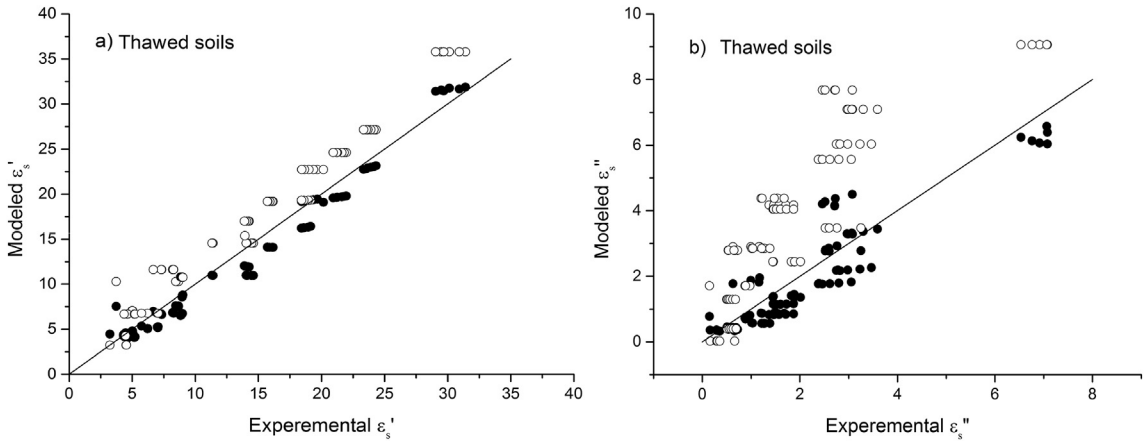

Fig. 7. The calculated CRPs of moist soils as a function of the measured ones for independent soils a) the real part of CRP, ε_s', b) the imaginary part of CRP, ε_s'', in the temperature ranges of $-0\ ^\circ C \le T \le 25\ ^\circ C$. Bisectors represented by the lines. Filled circles represent the earlier developed model (Mironov et al., 2013b), empty circles represent Dobson model.

Table 6
Statistical errors for the earlier developed model (***Mir***) and the Dobson model (***Dob***) in the case of thawed soils.

	Independent soils, $T > 0$					
	RMSE		nRMSE, %		R^2	
	Mir	Dob	Mir	Dob	Mir	Dob
ε_s'	1.54	2.79	12.29	22.29	0.96	0.90
ε_s''	0.65	2.41	33.41	181.31	0.84	0.42

developing either for the Mironov model or for the Dobson one. The results of comparison of calculations obtained with the use of the models in (Mironov et al., 2013b; Dobson et al., 1985) at positive temperatures with experimental data are shown in Figs. 4 and 5. As can be seen from these figures, the calculations with both models correlate well with the measured data. As to the real part of soils CRP, the Dobson model, as a rule, exceeds the experimental data, while the Mironov model slightly underestimates the measured ones. As to the imaginary part of soils CRP, the Dobson model substantially overestimates the experimental data, while the estimations with Mironov model perfectly follow the measured ones. The same relationship between the values of CRP calculated with the Dobson (empty circles) and Mironov (filled circles) models, on the one hand, and the measured ones, on the other hand, is demonstrated in Fig. 6, where the calculated CRP values are shown as a function of the respective measured ones for the broader variety of moistures. The statistical errors in terms of RMSE, nRMSE, and determination coefficient, concerning the measured and calculated data shown in Fig. 7 are presented in Table 6. As seen from Table 6 the values of nRMSE related to the Dobson model for the real and imaginary parts of soil CRPs exceed the respective values related to the Mironov model by factors of 2 and 5, respectively.

7. Conclusions

For the first time, the dielectric measurements for ***frozen*** mineral soils collected in the area of arctic tundra in Yamal peninsula were carried out in the range of temperatures $-30\ ^\circ C \le T \le -1\ ^\circ C$.

Based on these measurements, a single-frequency dielectric model at 1.4 GHz for frozen mineral soils was developed. Moreover, an integral dielectric model applied both for the frozen and thawed soils was suggested on the bases of the model for frozen soils developed in this research and the one for the thawed soils previously developed in (Mironov et al., 2013b). This integral single-frequency (1.4 GHz) dielectric model is applicable for predicting CRPs of moist mineral soils with gravimetric clay content up to 42%, and moistures varying from 0 to the field capacity in the range of temperatures $-30^\circ C \le T \le +25^\circ C$. The statistical errors of the developed integral model were estimated using the dielectric data especially measured for validation. The statistical errors of the developed integral dielectric model in terms of normalized RMSE for the real and imaginary parts of soil CRPs were found to be closed to the ones of the dielectric measurements. For the first time, the statistical errors of the only previously known dielectric model for frozen soils suggested in (Zhang et al., 2003) were estimated using the dielectric data measured in this research. The nRMSE estimations for the real and imaginary parts of the frozen soil CRPs for the Zhang dielectric model were found to be about three times as great compared to those of the dielectric model developed in this research. This feature of the developed model is expected to ensure more accurate remote sensing algorithms regarding the frozen soils. In particular, it may be useful as physical bases in the case of remote sensing algorithms which identify thawed or frozen state of the soil cover. In further research, additional dielectric measurements for frozen soils should be conducted to extend the dielectric database for frozen mineral soils in terms of their texture variety.

Acknowledgment

The study was supported by a grant from the Russian Foundation for Basic Research (project № 16-05-00572).

References

Aubertin, G.M., Kardos, L.T., 1965. Root growth through porous media under controlled conditions. Proc. Soil Sci. Soc. Am. 29, 290–293.
Curtis, J.O., Weiss Jr., C.A., Everett, J.B., 1995. Effect of soil composition on dielectric properties. In: Technical Report EL-95-34.
Dobson, M.C., Ulaby, F.T., Hallikainen, M.T., El-Rayes, M.A., 1985. Microwave dielectric behavior of wet soil – part II: dielectric mixing models. IEEE Trans. Geosci. Remote Sens. 23 (1), 35–46.
Ersahin, S., Gunal, H., Kutlu, T., Yetgin, B., Coban, S., 2006. Estimating specific surface area and cation exchange capacity in soils using fractal dimension of particle-size distribution. Geoderma 136 (3/4), 588–597.
Mialon, A., Richaume, P., Leroux, D., Bircher, S., Al Bitar, A., Pellarin, T., Wigneron, J.-P., Kerr, Ya.H., 2015. Comparison of Dobson and Mironov dielectric models in the SMOS soil moisture retrieval algorithm. IEEE Trans. Geosci. Remote Sens. 53 (6), 3084–3094.
Mironov, V.L., Dobson, M.C., Kaupp, V.H., Komarov, S.A., Kleshchenko, V.N., 2004. Generalized refractive mixing dielectric model for moist soils. IEEE Trans. Geosci. Remote Sens. 42 (4), 773–785.
Mironov, V.L., Fomin, S.V., 2009a. Temperature dependable microwave dielectric model for moist soils. In: PIERS Proceedings, March 23–27, Beijing China, pp. 831–835.
Mironov, V.L., Fomin, S.V., 2009b. Temperature and mineralogy dependable model for microwave dielectric spectra of moist soils. In: PIERS Proceeding, August 18–21, Moscow, Russia, pp. 938–942.
Mironov, V.L., Kosolapova, L.G., Fomin, S.V., 2009. Physically and mineralogically based spectroscopic dielectric model for moist soils. IEEE Trans. Geosci. Remote Sens. 47 (7/1), 2059–2070.
Mironov, V.L., De Roo, R.D., Savin, I.V., 2010a. Temperature-dependable microwave dielectric model for an arctic soil. IEEE Trans. Geosci. Remote Sens. 48 (6), 2544–2556.

Mironov, V.L., Komarov, S.A., Lukin, Yu.I., Shatov, D.S., 2010b. A technique for measuring the frequency spectrum of the complex permittivity of soil. J. Commun. Technol. Electron. 55 (12), 1368–1373.

Mironov, V.L., Bobrov, P.P., Fomin, S.V., 2013a. Multirelaxation generalized refractive mixing dielectric model of moist soils. IEEE Geosci. Remote Sens. Lett. 10 (3), 603–606.

Mironov, V., Kerr, Y., Wigneron, J.-P., Kosolapova, L., Demontoux, F., 2013b. Temperature and texture dependent dielectric model for moist soils at 1.4 GHz. IEEE Geosci. Remote Sens. Lett. 10 (3), 419–423.

Mironov, V.L., Molostov, I.P., Lukin, Y.I., Karavaisky, A.Y., 2013c. Method of retrieving permittivity from S12 element of the waveguide scattering matrix. In: International Siberian Conference on Control and Communications (SIBCON). 12–13 September, Krasnoyarsk. 978-1-4799-1062-5/13 ©2013 IEEE.

Mironov, V.L., Muzalevskiy, K.V., Savin, I.V., 2013d. Retrieving temperature gradient in frozen active layer of Arctic tundra soils from radiothermal observations in L-band—theoretical modeling. J. Sel. Topics Appl. Earth Observ. Remote Sens. 6 (3), 1781–1785.

Mironov, V.L., Kerr, Ya., Kosolapova, L.G., Savin, I.V., Muzalevskiy, K.V., 2015. Temperature dependent dielectric model for an organic soil thawed and frozen at 1.4 GHz. IEEE J. Sel. Topics Appl. Earth Observ. Remote Sens. 8 (9), 4470–4477.

Mironov, V.L., Muzalevskiy, K.V., Ruzicka, Z., 2016. Retrieving profile temperatures in a frozen topsoil near the TFS, Alaska, based on SMOS brightness temperatures at the 1.4-GHz frequency. IEEE Trans. Geosci. Remote Sens. 54 (12), 7331–7338. http://dx.doi.org/10.1109/TGRS.2016.2599272.

Rautiainen, K., Lemmetyinen, J., Pulliainen, J., Vehviläinen, J., Drusch, M., Kontu, A., Kainulainen, J., Seppänen, J., 2012. L-band radiometer observations of soil processes in boreal and subarctic environments. IEEE Trans. Geosci. Remote Sens. 50 (5), 1498–1506.

Rautiainen, K., et al., 2016. SMOS prototype algorithm for detecting autumn soil freezing. Remote Sens. Environ. http://dx.doi.org/10.1016/j.rse.2016.01.012.

Stogryn, A., 1971. Equation for calibration the dielectric constant of saline water. In: IEEE Trans. Micriwave Theory Thech., MTT-19, pp. 733–736.

Wagner, N., Emmerich, K., Bonitz, F., Kupfer, K., 2011. Experimental investigations on the frequency and temperature dependent dielectric material properties of soil. IEEE Trans. Geosci. Remote Sens. 49 (7), 2518–2530.

Wang, J.R., Schmugge, T.J., 1980. An empirical model for the complex dielectric permittivity of soils as a function of water content. IEEE Trans. Geosci. Remote Sens. GE-18 (4), 288–295.

Xu, X., Oliphant, J.L., Tice, A.R., 1985. Soil-water potential, unfrozen water content and temperature. J. Glaciol. Geocryol. 7 (1), 1–14.

Xu, X., Dunbar, R.S., Derksen, C., Colliander, A., Kimball, J., Kim, Y., 2016. Landscape freeze/thaw products from soil moisture active/passive (SMAP) radar and radiometer data. In: IEEE IGARSS. 2016. pp. 132–135 (978-1-5090-3332-4/16).

Zhang, L., Shi, J., Zhang, Z., Zhao, K., 2003. The estimation of dielectric constant of frozen soil-water mixture at microwave bands. In: Proc. of IGARSS, 21–25 July 2003, Toulouse, France, pp. 2903–2905.

Zhang, L., Zhao, T., Jiang, L., Zhao, S., 2010. Estimate of phase transition water content in freeze–thaw process using microwave radiometer. IEEE Trans. Geosci. Remote Sens. 48 (12), 4248–4255.

Zhao, S., Zhang, L., Zhang, Y., Jiang, L., 2012. Microwave emission of soil freezing and thawing observed by a truck-mounted microwave radiometer. Int. J. Remote Sens. 33 (3), 860–871.